Preparation and Characterization of Polypropylene/Serpentine Composites

Semra Tan, Teoman Tincer

Department of Chemistry, Middle East Technical University, TR-06531 Ankara, Turkey

Received 20 July 2010; accepted 13 October 2010
DOI 10.1002/app.33604
Published online 24 February 2011 in Wiley Online Library (wileyonlinelibrary.com).

ABSTRACT: Composites of serpentine and polypropylene (PP) were prepared by twin-screw extrusion. Serpentine was collected as rocks from the Ankara–Beynam region and ground into powder with an average particle size of about 3 μm for composite production. Both as-received (rock) and powdered serpentine were characterized. A silane coupling agent (SCA), γ-aminopropyl triethoxy silane, was used for the surface treatment of serpentine. Mechanical properties of the composites were measured in terms of impact strength, elastic modulus, stress at yield, stress at break, and percentage strain at break. The addition of serpentine was found to have a profound effect on the reinforcement of the PP matrix. Because of the stronger interactions at the interphase induced by SCA treatment, mechanical properties were improved further in comparison with the untreated composites. Similar thermal and morphological behaviors were recorded for the composites with and without surface treatment. Thermal studies showed an increase in both melting temperature and percentage crystallinity of the composites. Scanning electron microscopy analysis revealed that homogeneous distribution of filler was observed at low filler contents, but a certain extent of agglomeration was also seen at high filler loadings. © 2011 Wiley Periodicals, Inc. J Appl Polym Sci 121: 846–854, 2011

Key words: composites; mechanical properties; polypropylene; (PP)

INTRODUCTION

Polypropylene (PP) is an industrially important polymer used in large number of applications because of its attractive properties, such as ease of processability, high stiffness at low density, and good resistance to chemicals, fatigue, and environmental stress cracking. Modification of the resin is an important consideration to achieve better physical and mechanical properties and to extend the diversity of end products. Commonly, inorganic fillers and short glass fibers are used to improve the mechanical properties of polyolefins. Talc and calcium carbonate are the two mostly used fillers in PP matrices.[1–3] Although talc[4,5] provides mainly an increase in stiffness and thermal conductivity, $CaCO_3$[6] increases the toughness of PP resins. Furthermore, the followings have been used and studied as fillers and also for some special purposes: glass fibers,[7] mica,[8] glass beads,[9] perlite,[10] magnesium hydroxide,[11] wood flour,[12] and cellulose.[13] Carbon black, steel fibers and metal powders, especially of aluminum, iron, and nickel, have also been applied to improve the electrical and magnetic properties of PP.[14]

The filler characteristics, such as surface of the filler, particle type, purity, size, and aspect ratio have an important role in determining the composite properties. Mostly, treatment of the filler surface is required to improve the coupling of the continuous and dispersed phases.[14] Maiti and Sharma[15] investigated the effect of surface treatment of talc with a titanate coupling agent on the tensile and impact properties of PP/talc composites with up to 60 wt % talc content. They obtained better mechanical properties in the presence of a coupling agent. Leong et al.[16] studied the effects of different filler treatments on the mechanical, flow, thermal, and morphological properties of PP/$CaCO_3$ composites. They observed that with the use of silane and titanate coupling agents, both the elongation at break and impact strength of the composites were improved.

Serpentine was chosen as the filler in this study because of its abundance and low cost. The massive serpentine, translucent and light to dark green in color, can be used as an ornamental stone and building material, as a flux in iron and steel production, as filler for road pavement, and as floor material for construction.[17–19] There are basically three different polymorphs, antigorite, lizardite, and chrysotile. Antigorite has a slightly different composition than other serpentine varieties. It has a modulated structure that relieves the bad fit between the layers most

Correspondence to: T. Tincer (teotin@metu.edu.tr).

effectively.[20] Lizardites are extremely fine-grained platy minerals with layers of different orientations. The structure is planar, in which the tetrahedral (T) sheet is distorted to match the corresponding octahedral (O) sheet.[21,22] In chrysotile, the structure somewhat resembles that of antigorite if one assumes a cylindrical curvature along the fiber axis in which expanding layers lead to the formation of fibers.[22,23]

Serpentine, with an approximate formula of $Mg_3Si_2O_5(OH)_4$, belongs to the same family of silicates as talc, mica, and montmorillonites. It is made up of O and T sheets that are combined to form layers and is classified in accordance with how the sheets are combined, i.e., T and O sheet (T–O type) or two T sheets outside of an internal O sheet (T–O–T type). The stacking of the layers is maintained with weak van der Waals forces if the interlayers are neutral. Otherwise, in the case of a charge imbalance in either sheet because of substitutions, the cations between the layers hold them together.[24,25] In the last two decades, montmorillonites, being T–O–T type phyllosilicates, have been the most suitable and successful fillers in the production of nanocomposites.[26,27]

In this study, the objective was to explore the characteristics of serpentine as a filler in PP/serpentine composites. The surface treatment of serpentine was performed by a silane coupling agent (SCA). Effort was focused on grinding of serpentine rock into powder, addition into the PP matrix, and study of mechanical, thermal, and morphological properties of the resultant composites.

EXPERIMENTAL

Materials

HE125MO 25308 grade PP, with a melt mass flow rate of 12.0 g/10 min (230°C/2.16 kg) and a specific gravity of 0.908, was purchased from Borealis AG (Vienna, Austria). Serpentine of the Ankara–Beynam region (40 km south of Ankara), collected as rocks, was used as the filler. The characteristics of serpentine, both as-received and after it was milled into the powder form, were studied before processing of the composites. The SCA of γ-aminopropyl triethoxy silane (A-1100), an early product of Union Carbide (Hahnville, LA), was used as the surface modifier (Fig. 1).

Powder serpentine production and characterization

Serpentine rocks were hammered to small pieces, ground, rolled, and pulverized to produce powdered filler. Pulverized powders were wet-sieved with ethanol by a 400-mesh (<38 μm) sieve. After the removal of ethanol, ball milling was carried out to obtain serpentine powders as small as possible in size without the use of any dispersants. We performed wet milling in a 1800-mL hardened porcelain jar containing stainless steel balls with ethanol at a ball-to-powder ratio of 10 by holding the weights of the filler and balls at 350 and 3500 g, respectively, for 48 h. The powders were kept in muffle furnace for 3 days at 350°C for drying.

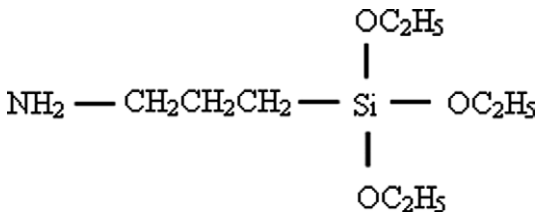

Figure 1 Structure of A-1100 (γ-aminopropyl triethoxy silane).

A number of tests were used to characterize the filler because of the presence of different serpentine varieties all over the world. The specific gravity of serpentine was measured by an Alfa Mirage electronic densimeter MD-300S (Osaka, Japan). X-ray analysis was performed on powdered serpentine by a Rigaku D/Max 2200/PC X-ray diffractometer (Tokyo, Japan) by the application of Cu Kα radiation with $\lambda = 1.54$ Å, 40 kV, and a 40-mA source. The diffraction pattern was recorded at a scanning rate of 1°/min and with steps of 0.01°. The morphological characteristics of the powdered serpentine were analyzed by a JEOL JSM-840A SM (Tokyo, Japan). Differential thermal analysis (DTA)/thermogravimetry (TG) analysis was conducted in air and nitrogen atmospheres at a heating rate of 10°C/min between 50 and 850°C by a Setaram Labsys thermogravimetric analysis/DTA instrument (Caluire, France). Thin sections of a serpentine sample were examined by an Olympus BH-2 type microscope (Center Valley, PA) at a magnification of 40×. The particle size measurement after milling was carried out by a Malvern Mastersizer 2000 (Worcestershire, United Kingdom) in ethanol medium. The surface area was measured with a gas (N_2) adsorption technique by a Quantachrome Corp. Autosorb-1-C/MS (Boynton Beach, FL).

Preparation of the composites

PP/serpentine composites were grouped into untreated and treated (with SCA). All serpentine powders were dried in a furnace at 350°C overnight before they were used as fillers with or without treatment. SCA was dissolved in diethyl ether, and the filler was added with well mixing at a 1 : 46 weight ratio of SCA to serpentine. The powders were dried overnight at 100°C to remove diethyl ether and to get rid of any moisture. Composites with 2, 5, 10, and 20% serpentine by weight were prepared (Table I) by a Thermoprism TSE 16 TC

TABLE I
Names of the Composites

Composite	PP (wt %)	Serpentine (wt %)	SCA treatment[a]
PP	100	—	—
PPS2	98	2	—
PPS5	95	5	—
PPS10	90	10	—
PPS20	80	20	—
PPS–Sil2	98	2	*x*
PPS–Sil5	95	5	*x*
PPS–Sil10	90	10	*x*
PPS–Sil20	80	20	*x*

[a] *x* indicates that the filler treatment was performed.

(Newington, NH) corotating, intermeshing, twin-screw extruder (diameter = 16 mm, length = 384 mm) at a screw speed of 190 rpm. The barrel temperature was 220°C from hopper to die, and the feed rate was 20 g/min. One-step extrusion was carried out. Whereas PP was fed into the extruder from the main feeder, serpentine was fed from the side feeder. After they were pelletized and dried at 80°C, the extruded samples were shaped by an Arburg Allrounder 220-90-350 type injection molding machine (Lossburg, Germany). The barrel temperatures were adjusted to 200, 220, 240, and 250°C. The mold temperature was kept at about 30°C.

Characterization of the composites

PP/serpentine composites were characterized by mechanical, thermal, and morphological examinations. Tensile testing was performed by an Instron tensile testing machine TM1102 (Norwood, MA) on standard, dumbbell-shaped injection-molded samples according to ASTM D 638. The crosshead speed and gauge length were 50 mm/min and 75 mm, respectively. Unnotched Charpy impact testing was used on injection-molded samples 70 × 7 × 2 mm^3 in size by a Pendulum impact tester type Coesfeld Material Test machine (Dortmund, Germany) according to ASTM D 256. All mechanical testing was carried out on at least seven samples for each composition, and the average results were reported at room temperature. Scanning electron microscopy (SEM) analysis was performed on the impact fractured surfaces of the samples by a JEOL JSM 6400 SM (Tokyo, Japan) and an FEI Quanta 400 field emission scanning electron microscope (Hillsboro, OR) to study the morphological properties. Thermal analyses were carried out between 20 and 200°C under a nitrogen atmosphere at a heating rate of 10°C/min by a DuPont Thermal Analyst 2000 DSC 910 S (New Castle, DE). The percentage crystallinity of PP in the composites was calculated according to the following equations with the volume fraction of PP considered:

ΔH = Melting enthalpy from the thermogram (J/g)/PP ratio

$$\text{Crystallinity}\,(\%) = (\Delta H/\Delta H_{100}) \times 100$$

where ΔH_{100} is 209 J/g[28] and represents the heat of fusion for a 100% crystalline PP.

RESULTS AND DISCUSSION

Characterization of serpentine

The X-ray diffraction (XRD) pattern of the powder (coarse-ground, as-received, and milled) samples displayed characteristic peaks belonging to serpentine minerals. As the pattern in Figure 2 indicates, the serpentine contains lizardite (the main constituent) and chrysotile together. The morphology of the as-received serpentine studied by SEM revealed that as-collected pieces have a platelet morphology, which confirms the lizardite-based structure (Fig. 3). They agglomerated [Fig. 3(b)] but easily disintegrated into smaller particles (i.e., average size ≈ 3 μm). Long fibers of asbestiform chrysotile were not observed in the serpentine samples. Figure 4(a) shows serpentine in its natural color, as brown with dark iron oxide regions. The mesh texture with characteristic birefringence colors of serpentine is illustrated in Figure 4(b). X-ray analysis carried out after ball milling showed that there was no change in the crystal structure of serpentine (Fig. 5). Meanwhile, the following characteristics were measured and determined to characterize the serpentine used as a filler: specific gravity = 2.5, Brunauer–Emmett–Teller surface area = 61.2 m^2/g, and volume-based average particle size [d(0.5)] = 3.2 ± 1.0 μm.

Thermal properties of the as-received serpentine were measured in air and nitrogen atmospheres.

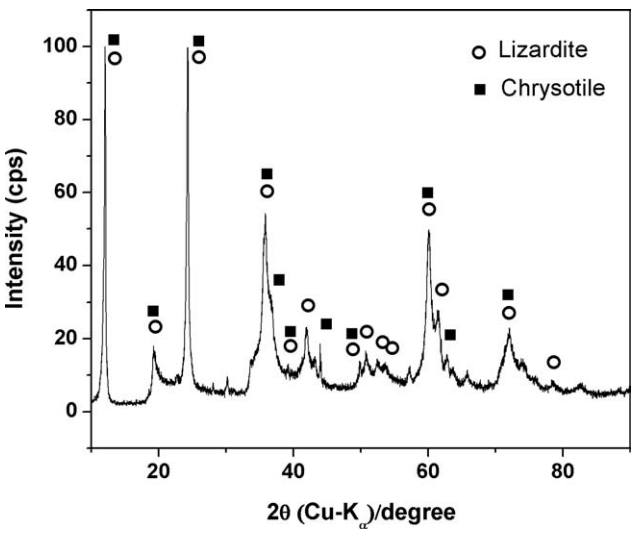

Figure 2 XRD pattern of the as-received serpentine mineral.

Analysis of the DTA curves showed three endothermic peaks at about 200 and 400°C due to the release of free and bound water, and the dehydroxylation of serpentine was assigned to 650°C, as given in Figure 6. Further heating caused serpentine to show an additional exothermic peak at about 820°C due to forsterite crystallization.

Mechanical properties of the composites

Impact strength

It is generally true that the incorporation of mineral fillers to polymers does not improve the impact strength of the matrices. Accordingly, the overall view of the results shows that introduction of the filler resulted in a decrease in the impact strength of neat PP. Upon the increase in filler loading, the impact strength continued to decrease for both treated and untreated composites (Fig. 7). However, it seemed that serpentine, even at high loadings, did not cause a big change in the impact strength of the

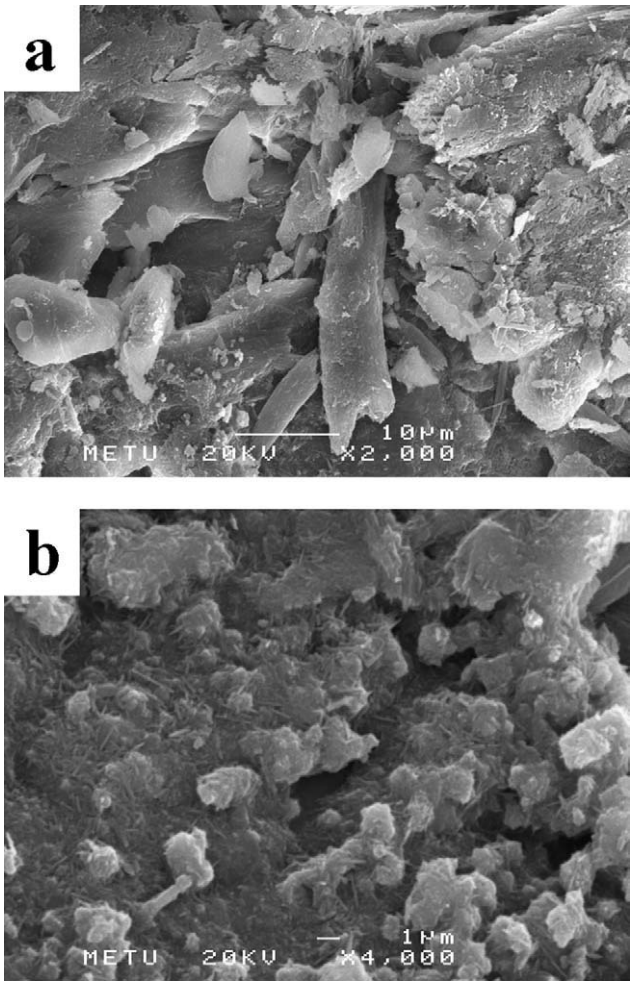

Figure 3 SEM pictures of the as-received serpentine at magnifications of (a) 2000 and (b) 4000×.

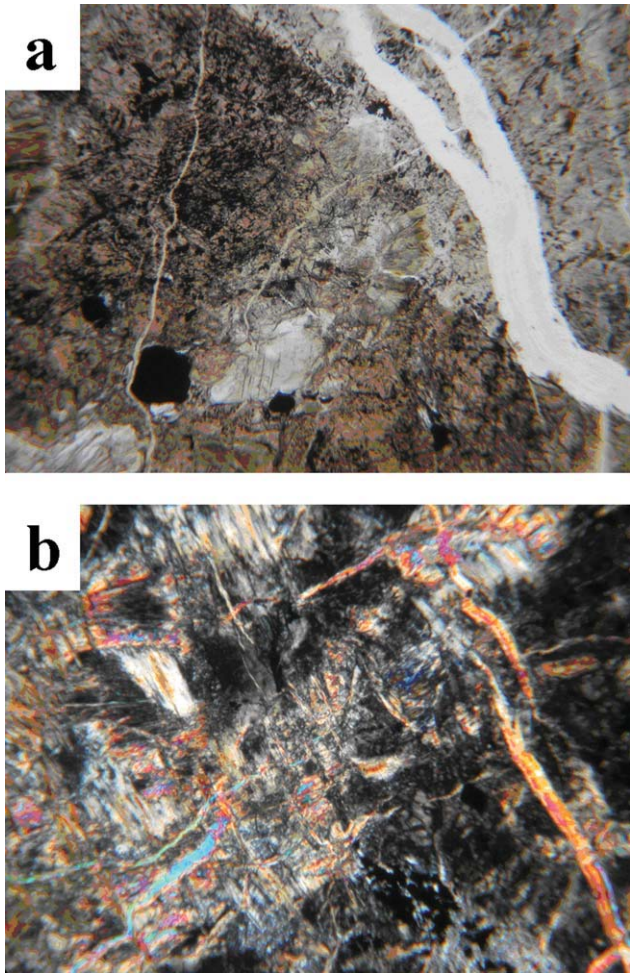

Figure 4 Thin-section photographs of the serpentine at 40× magnification: views under (a) plain, polarized light and (b) cross-polarized light. [Color figure can be viewed in the online issue, which is available at wileyonlinelibrary.com.]

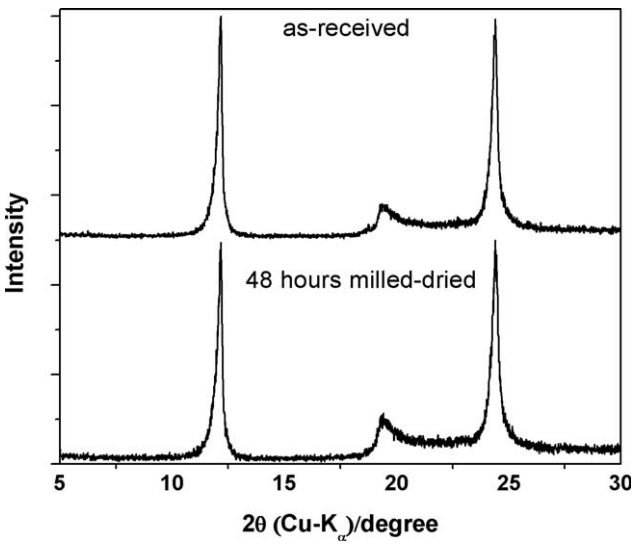

Figure 5 XRD patterns of the untreated, as-received serpentine and milled-powder serpentine (the pattern for the as-received sample was shifted for clarity).

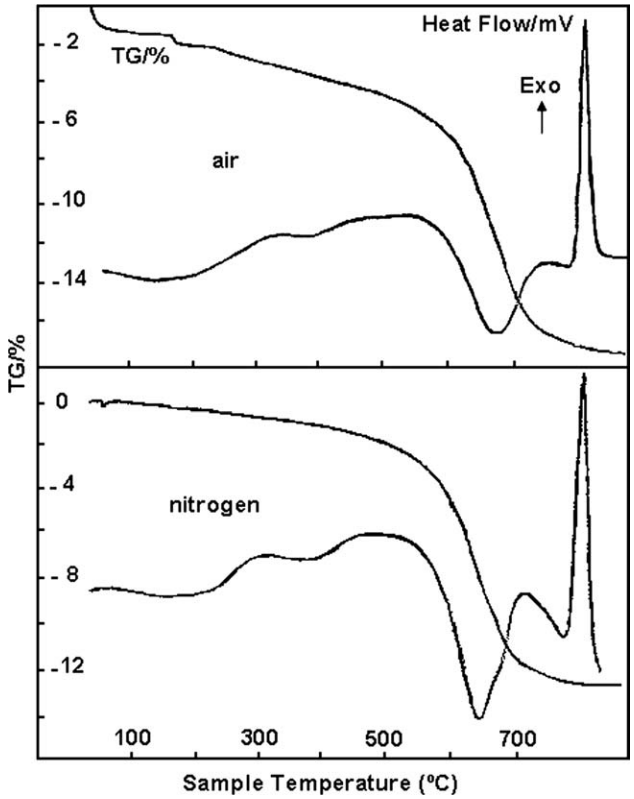

Figure 6 DTA/TG curves of serpentine in air and nitrogen.

composites compared to some other fillers, such as glass beads and mica.[29–31]

An increase in the filler content reduced the deformability of the matrix, and the resulting composite absorbed less energy before break. One important parameter determining the impact properties of the composites was the polymer–filler interaction. Accordingly, we expected that the SCA-treated composites would show higher impact strength than the untreated ones. As shown in Figure 7, the effect of SCA treatment on the impact strength of the PP/serpentine composites changed, depending on the filler amount. At low concentrations (2 and 5 wt % serpentine addition), SCA improved the impact strength, which was measured as 27.7 and 23.1 kJ/m^2 for SCA composite (PPS–Sil2, where the number indicates the weight percentage of serpentine) and untreated composite (PPS2, where the number indicates the weight percentage of serpentine), respectively. At high filler loadings, SCA did not show any distinguishable differences in the impact strength, as was observed for the 2 and 5 wt % serpentine-filled composites.

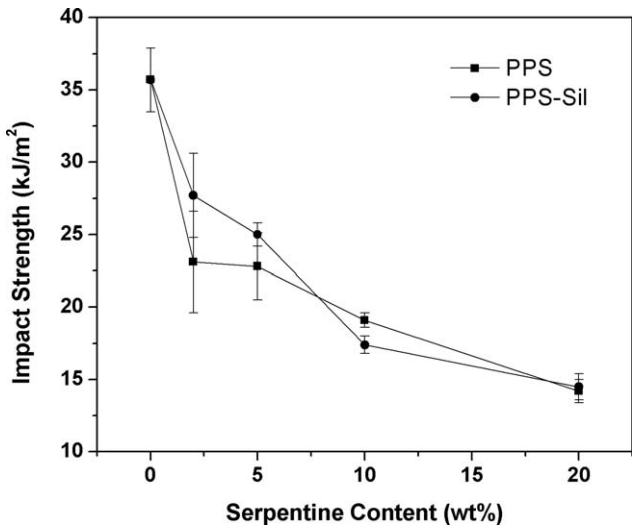

Figure 7 Variation of the impact strength of the PP/serpentine composites (with and without SCA) with the serpentine content (each data point is shown with its standard deviation).

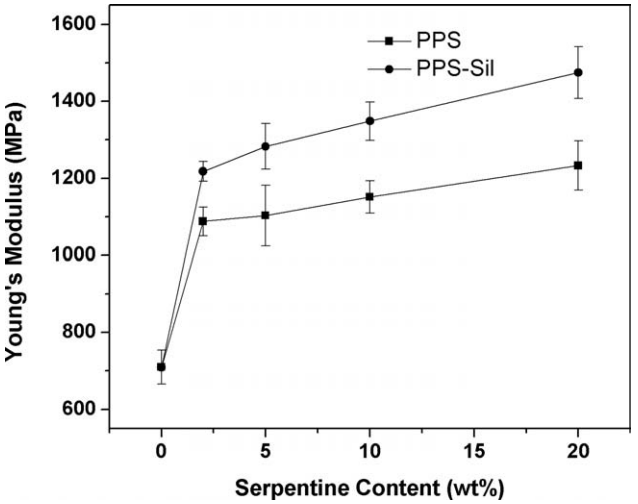

Figure 8 Variation of the Young's modulus of the PP/serpentine composites (with and without SCA) with the serpentine content.

Tensile testing

The tensile properties were evaluated through the study of the Young's modulus, stress at yield, stress at break, and percentage strain at break. Figure 8 illustrates the variation of Young's modulus with the filler concentration and treatment. There was a significant improvement in the modulus as the filler content increased for both composite types. The increases realized were 53.2% for PPS2, 55.4% for PPS5, 62.1% for PPS10, and 73.7% for PPS20, as compared to the modulus of neat PP. This increment was attributed to the good reinforcing ability of serpentine for PP. The use of rigid inorganic fillers leads to an increase in the modulus because of the restriction of the deformability of the matrix imposed by the filler. The movements of polymer chains through each other are hindered by filler

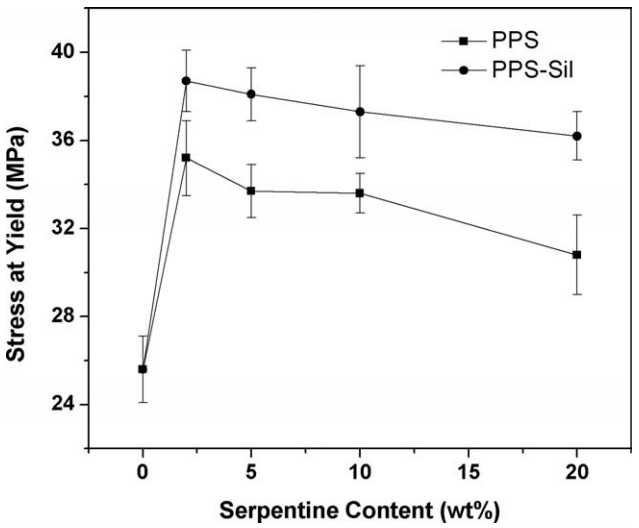

Figure 9 Variation of the stress at yield of the PP/serpentine composites (with and without SCA) with the serpentine content.

constraints. Although from the lowest to the highest filler contents, the modulus increased gradually, regardless of filler treatment, in the presence of SCA, the increase was more pronounced. Upon the incorporation of 20 wt % filler, whereas the maximum modulus attained for the untreated composites was 1233 MPa (a 73.7% increase over neat PP), it was 1475 MPa (a 107.7% increase over neat PP) for the treated composites. In the presence of SCA, because of the improvement of the interphase, the mobility and, therefore, deformability were much more prevented; this caused a higher modulus in comparison to the untreated composites. Moreover, the platelet shape of serpentine may have also contributed to the high modulus of the composites.

The yield stress of the composites is presented in Figure 9. Interfacial interactions are much more important in yield stress than in the elastic modulus because the former is measured at relatively higher deformations than the latter.[32,33] SCA treatment clearly showed its effect as an increment in stress at yield values compared to untreated composites because of the interphase improvement. The platelet geometry of serpentine and agglomeration at high filler amounts may have been effective and led to a low yield stress due to the possible increase in the stress concentration at the interphase during tensile testing. Although the stress at yield decreased from a low filler content to a high filler content, all stress at yield values were found to be higher than neat PP. The homogeneity of the continuous phase was not greatly influenced with the presence of the filler. However, the yield stress decreased with filler because of loss of ductility and a decrease in homogeneity. Consequently, lower yield stress values were observed at high filler amounts, and this was attributed to the presence and distribution of the serpentine filler.

The ultimate tensile properties of PP/serpentine composites are presented through the stress at break and percentage strain at break graphs. The stress at break values changed in a similar manner as the stress at yield (Fig. 10). By the application of filler, the stress at break of PP increased to 34.5 and 37.5 from 21.9 MPa for PPS2 and PPS–Sil2, respectively. Higher stress at break values were recorded for the SCA-treated composites than for the untreated composites. Although the results obtained for both composite types indicated a decreasing trend from 2 to 20 wt % filler, they were still well above the stress at break of neat PP.

The variations in the elongation at break of the untreated and treated composites are given in Figure 11. The incorporation of 2 wt % serpentine, either untreated or treated, caused a very drastic reduction in the elongation at break of neat PP, which was recorded as 367.6. This value decreased to 10 and 6.9 for PPS2 and PPS–Sil2, respectively. With the increase in the solid undeformable phase in the matrix, the elongation at break continued to decrease for composites with and without SCA. However, the reduction on going from 2 to 20 wt % filler addition was not tremendous; on the contrary, it was very slow. SCA-treated composites showed a lower elongation at break than the untreated composites. This result once more showed the coupling effect of SCA. Because the matrix deformability was limited in the presence of filler, very low values of the elongation at break of the PP composites were recorded.

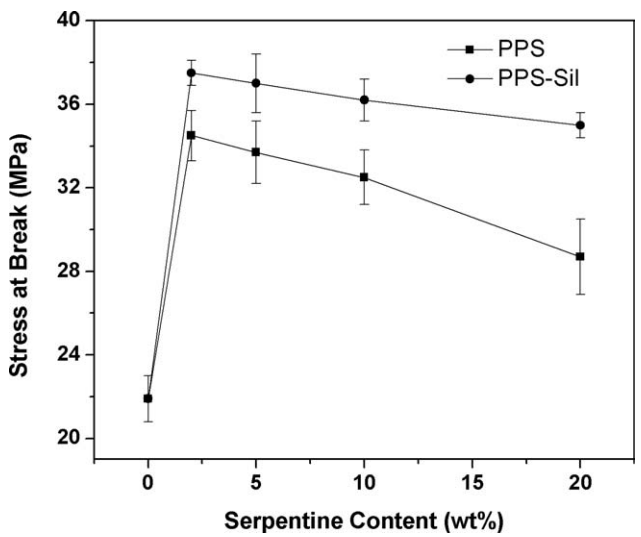

Figure 10 Variation of the stress at break of the PP/serpentine composites (with and without SCA) with the serpentine content.

Thermal behavior and crystallinity of the matrices

The melting temperatures and the percentage crystallinity of composites were followed by differential scanning calorimetry, as given in Table II. An upward shift of 1–3°C in the melting temperatures was observed for the composites in comparison to PP. This increase was correlated to the reduction in the chain mobility of the polymer chains, which led to a more stabilized matrix and the melting of the crystal structure at higher temperatures. One possible explanation for the higher melting temperatures of the composites is a probable increase in the lamellar thickness of the PP crystals. Furthermore, the onset melting temperatures of the PP/serpentine composites were found to be 2–3°C lower than that of PP, with one exception, but this was within the experimental error limits. With the decrease in the onset melting temperature, the melting range increased. This might be an indication of the presence of imperfect crystals in the composite. Evidently, these changes showed an increased melting range (from onset to melting temperatures) for the filled samples. Then, the percentage crystallinity, especially at high loadings, was higher than that of PP. No significant differences in the melting behavior and percentage crystallinity were observed for SCA-treated composites compared to untreated ones. In general, we concluded that the serpentine may have acted as a nucleating filler; this led to heterogeneous nucleation and an increase in the percentage crystallinity.

Morphology of the composites

To follow the variations in the morphology of the composites, SEM analysis was used. Figure 12 gives the SEM images of the impact-fractured surfaces of untreated and treated composites at serpentine loadings of 2 and 10 wt %. An overview of the images shows that serpentine did not greatly alter the fracture morphology of PP. The PPS2 and PPS–Sil2 composites showed a fine distribution throughout the matrix, as seen in Figure 12(a,c). Accompanying the increase in filler content, agglomerated filler portions were observed. The SEM micrographs [Fig. 12(b,d)] of PP10 and PP10S showed both homogeneous particles and aggregated phases together. A comparison of the SEM observations indicated that the SCA treatment had no influence on the distribution behavior of serpentine through the matrix, but it improved adhesion, which caused better mechanical properties. However, a smooth and ductile fracture was observed in both the SCA-treated and untreated serpentine-filled samples.

TABLE II
Onset and Peak Melting Temperatures (T_m's) and Crystallinity of the Composites

	T_m (°C)		
Composite	Onset	Peak	Crystallinity (%)
PP	156.4	167.0	29.76
PPS2	154.6	168.1	30.31
PPS5	154.3	170.1	28.87
PPS10	154.3	169.6	35.73
PPS20	153.9	167.9	36.02
PPS–Sil2	154.7	170.2	34.32
PPS–Sil5	155.0	168.1	35.59
PPS–Sil10	154.3	169.7	33.14
PPS–Sil20	156.9	168.5	31.18

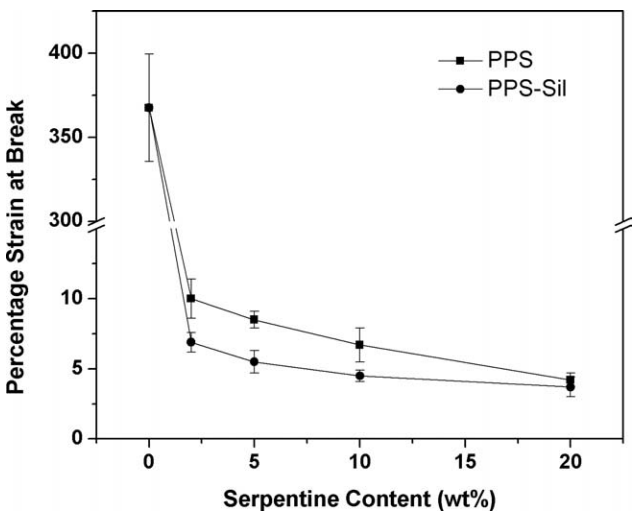

Figure 11 Variation of the strain at break (%) of the PP/serpentine composites (with and without SCA) with the serpentine content.

CONCLUSIONS

Serpentine as a filler, with an average particle size of about 3 μm, was successfully introduced into the PP matrix. Serpentine addition led to improvements in the tensile properties of the composites. Even with the addition of 2 wt % serpentine, the elastic modulus of PP was improved by 53.2%. All of the studied filler loadings caused an increase in both yield stress and stress at break values of PP matrix. This indicates good adhesion between the matrix and the filler when the hydrophobic nature of PP and the hydrophilic nature of serpentine were concerned. Although untreated serpentine proved to be a suitable candidate for PP composites exhibiting very good mechanical properties, further improvements were observed for the SCA-treated composites. The impact strength of the treated composites at low filler contents was higher than that of the untreated ones. However, it was clear that after that, SCA treatment did not cause any important changes in

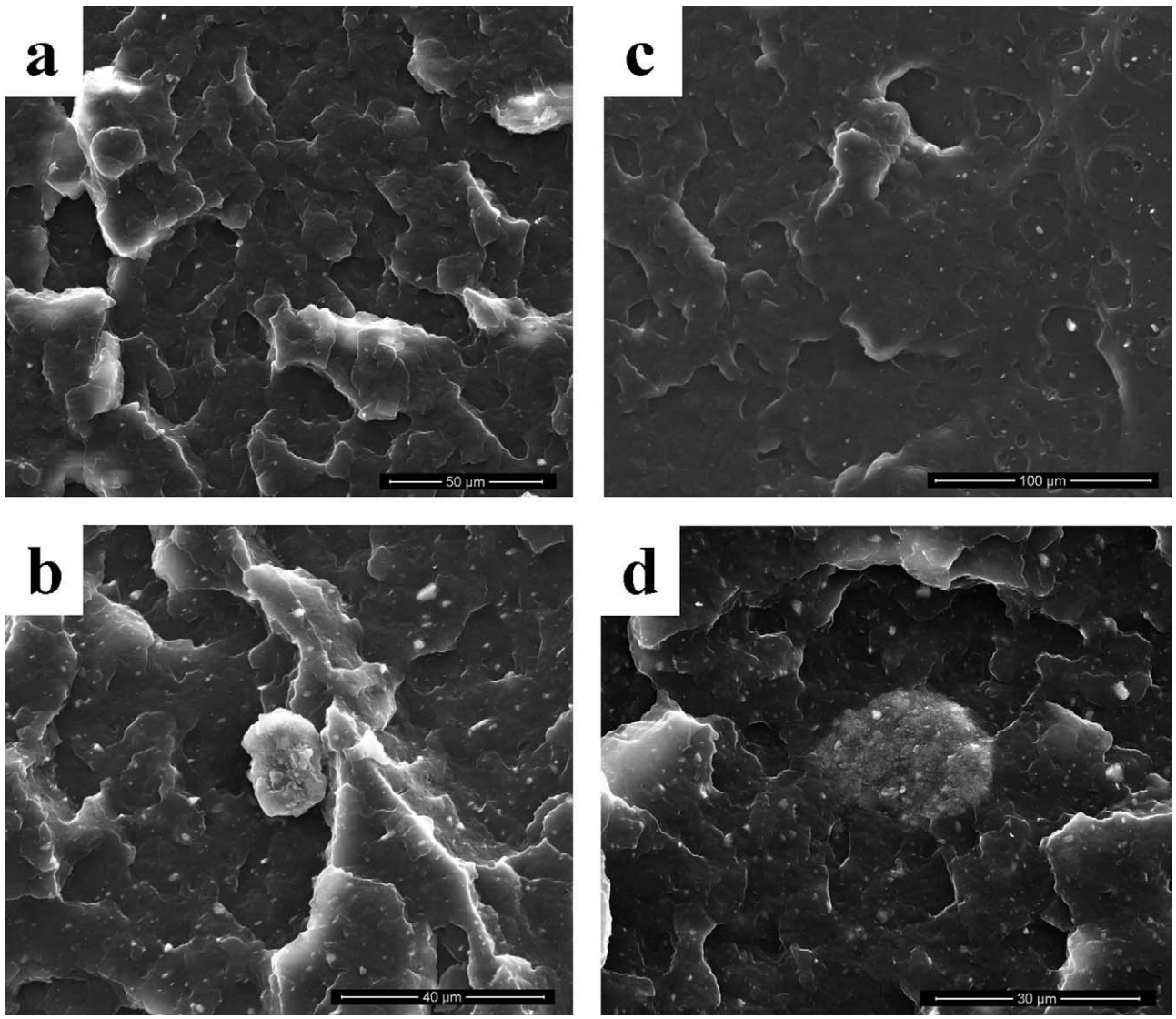

Figure 12 SEM micrographs of the impact-fractured surfaces of (a) PPS2 (1600×), (b) PPS10 (2650×), (c) PPS–Sil2 (1130×), and (d) PPS–Sil10 (3550×).

the impact strength. The elastic was improved more at all filler loadings showing an increased reinforcing effect of serpentine. Moreover, the stress at yield and stress at break values also increased with SCA because of enhanced interactions in these composites. Percentage strain at break values of treated composites were lower than those of untreated ones, which is another evidence of the improved adhesion at the interphase.

Differential scanning calorimetry results show that in the presence of serpentine, the melting points of the composites increased up to 3°C, and the crystallinity of the composites also increased because of the nucleating effect of the serpentine. The morphological studies showed that depending on the amount of filler, its dispersion through the matrix changed. Although, at low filler contents, a homogeneous distribution was attained, at high filler contents, both well-distributed particles and aggregated filler portions were observed. Similar melting behavior, percentage crystallinity, and morphology were attained for both types of composites produced.

In the overall scheme, serpentine could be a new, proper choice for reinforcing PP. It is possible to say that for the studied filler loading range, the mechanical properties were somewhat independent of filler content because just after the addition of 2 wt % serpentine, any big changes in the measured values were not observed. SCA treatment, without any doubt, produced a better harmony between serpentine and PP. To conclude, serpentine seems to be a very good candidate as filler for PP, in terms of its effect both in reinforcing the polymer and reducing the production costs.

References

1. Rothon, R. N. Particulate Fillers for Polymers; Vol. 12 No. 9; Rapra Technology: Shawbury, England, 2002.
2. Frank, H. P. Polypropylene; Gordon and Breach Science: New York, 1968.
3. Nielsen, L. E. Mechanical Properties of Polymers and Composites; Marcel Dekker: New York, 1974; Vols. 1–2.
4. Karian, H. G. Handbook of Polypropylene and Polypropylene Composites; Marcel Dekker: New York, 2003.
5. Weidenfeller, B.; Höfer, M.; Schilling, F. R. Compos A 2004, 35, 423.
6. Leong, Y. W.; Abu Bakar, M. B.; Ishak, Z. A. M.; Ariffin, A.; Pukanszky, B. J Appl Polym Sci 2001, 91, 3315.
7. Sova, M.; Pelzbauer, Z. J Appl Polym Sci 1989, 38, 511.
8. Trotignon, J. P.; Sanschagrin, B.; Piperaud, M.; Verdu, J. Polym Compos 1982, 3, 230.
9. Liang, J. Z. Macromol Mater Eng 2001, 286, 714.
10. Akin-Oktem, G.; Tanrisinibilir, S.; Tincer, T J Appl Polym Sci 2001, 81, 2607.
11. Chen, X. L.; Yu, J.; Guo, S. Y. J Appl Polym Sci 2006, 102, 4943.
12. Nachtigall, S. M. B.; Cerveira, G. S.; Rosa, S. M. L. Polym Test 2007, 26, 619.
13. Zugenmaier, P. Pure Appl Chem 2006, 78, 1843.
14. Kocsis, J. K. Polypropylene Structure, Blends and Composites. Vol. 3. Composites; Chapman & Hall: Cambridge, England, 1995.
15. Maiti, S. N.; Sharma, K. K. J Mater Sci 1992, 25, 4605.
16. Leong, Y. W.; Abu Bakar, M. B.; Ishak, Z. A. M.; Ariffin, A. J Appl Polym Sci 2005, 98, 413.
17. Klein, C.; Hurlbut, C. S. Manuel of Mineralogy; Wiley: New York, 1993.
18. Zhang, Q.; Sugiyama, K.; Saito, F. Hydrometallurgy 1997, 45, 323.
19. Kim, D. J.; Chung, H. S. Part Sci Technol 2002, 20, 158.
20. Ernst, W. G. Serpentine and Serpentinites: Mineralogy, Petrology, Geochemistry, Ecology, Geophysics, and Tectonics; Bellwhether: Columbia, 2004.
21. Deer, W. A.; Howie, R. A.; Zussman, J. An Introduction to the Rock Forming Minerals; Longman: New York, 1966.
22. Nesse, W. D. Introduction to Mineralogy; Oxford University Press: New York, 2000.
23. Bailey, S. W. Hydrous Phyllosilicates: Exclusive of Micas; Mineralogical Society of America Book Crafters: Washington, DC, 1988.
24. Wenk, H. R.; Bulakh, A. Minerals—Their Constitution and Origin; Cambridge University Press: Cambridge, England, 2004.
25. Putnis, A. Introduction to Mineral Sciences; Cambridge University Press: Cambridge, England, 1992.
26. Varela, C.; Rosales, C.; Perera, R.; Matos, M.; Poirier, T.; Blunda, J.; Rojas, H. Polym Compos 2006, 27, 451.
27. Marchant, D.; Jayaraman, K. Ind Eng Chem Res 2002, 41, 6402.
28. Brandrup, J.; Immergut, E. H. Polymer Handbook; Wiley-Interscience: New York, 1989.
29. Denault, J.; Vu-Khanh, T. Polym Compos 1988, 9, 360.
30. Liebowitz, H. Fracture; Academic: New York, 1968.
31. Busigin, C.; Lahtinen, R.; Martinez, G. M.; Thomas, G.; Woodhams, R. T. Polym Eng Sci 1984, 24, 169.
32. Stricker, F.; Bruch, M.; Mülhaupt, R. Polymer 1997, 38, 5347.
33. Pukanszky, B. Composites 1990, 21, 255.